Journal of Organometallic Chemistry 921 (2020) 121332

Contents lists available at ScienceDirect

Journal of Organometallic Chemistry

journal homepage: www.elsevier.com/locate/jorganchem

Backbone effects in the synthesis, coordination chemistry and catalytic properties of new chiral heterobidentate ligands with P,N and S,N donor sets

Máté M. Major [a], Zsófia Császár [a], Attila C. Bényei [b], Szabolcs Balogh [c], József Bakos [a], Gergely Farkas [a, *]

[a] University of Pannonia, Department of Organic Chemistry, H-8200, Veszprém, Egyetem u. 10, Hungary
[b] University of Debrecen, Department of Pharmaceutical Chemistry, Egyetem tér 1, H-4032 Debrecen, Hungary
[c] University of Pannonia, NMR Laboratory, H-8200, Veszprém, Egyetem u. 10, Hungary

ARTICLE INFO

Article history:
Received 26 February 2020
Accepted 29 April 2020
Available online 20 May 2020

Keywords:
Chelate ring size
Heterobidentate
Asymmetric catalysis
Palladium
Allylic alkylation

ABSTRACT

Novel alkane-diyl based heterobidentate P,N and S,N ligands with the general formula $R^1R^2NCH(R^3)(CH_2)_nCH(R^4)Q$ (R^1 = Me or *i*Pr; R^2 = H or Me; R^3, R^4 = H or Me; n = 0, 2; Q = PPh_2 or SPh) have been prepared starting from cyclic sulfate esters or naturally occurring compounds with C_1 symmetry. The length of the ligands' backbone and the reaction conditions applied strongly affected the stereochemical outcome of the synthesis when using cyclic sulfates as starting materials. Palladium(II)-complexes of the new ligands were characterized by 1D and 2D NMR spectroscopy in solution and in several cases by X-ray crystallography in the solid phase. The structural versatility of the ligands enabled the straightforward comparison of the stereoselectivity of their coordination as a function of their tether length, backbone substitution pattern, donor sets and relative carbon atom configuration in their backbone. The catalytic features of the novel compounds were investigated in asymmetric allylic alkylation reactions where the tether length proved to be a crucial factor in determining enantioselectivity.

© 2020 The Authors. Published by Elsevier B.V. This is an open access article under the CC BY-NC-ND license (http://creativecommons.org/licenses/by-nc-nd/4.0/).

1. Introduction

Homogeneous transition metal catalysis represents a powerful tool in synthetic organic chemistry and its relevance continuously increases [1]. Higher atom economy, activity and selectivity can be achieved or more complicated reaction sequences can be substituted by simple catalytic steps [2]. It is, therefore, not surprising that the design and synthesis of novel transition metal catalysts (ligands) providing high activity and (enantio)selectivity is a fundamental requirement for further progress in this field.

In the past few decades, the exploration of ligand effects in transition metal catalysis became a powerful tool for the fine tuning of the catalyst's structure to improve its efficiency in homogeneous systems [3]. In asymmetric transition metal catalysis, the majority of reports on ligand modifications have followed systematic variation of the simple spatial demands of the catalyst [4], and substituent controlled electronic tuning of the chiral ligands [5]. Less common are instances of the manipulation of the chelate ring size, despite the fact that such changes can be, in many cases, readily implemented resulting in steric and also electronic alteration and producing similarly dramatic improvements in catalytic activity and enantioselectivity [6]. Accordingly, the variation of the chelate ring size might strongly influences the (i) electronic properties of the donoratoms, (ii) the bite angle of the chelate complex, (iii) the spatial position of the terminally disposed donoratom substituents as well as (iv) the conformational flexibility of the chelate. Furthermore, in the case of chiral heterodonor ligands with non-persistent donoratom chirality (v) the hemilability of the chelate ring and (vi) the stereoselectivity of the donoratom coordination can also depend on the ring size.

Chiral bidentate ligands in which different donoratoms are employed represent a unique class of compounds in asymmetric catalysis. The potential of such ligands mainly arises from the rather distinct electronic and steric differentiation of the coordinating functionalities. In this context, P,N [7] and S,N [8] ligands can be

* Corresponding author.
E-mail address: gerifarkas@almos.uni-pannon.hu (G. Farkas).

https://doi.org/10.1016/j.jorganchem.2020.121332
0022-328X/© 2020 The Authors. Published by Elsevier B.V. This is an open access article under the CC BY-NC-ND license (http://creativecommons.org/licenses/by-nc-nd/4.0/).

mentioned as highly effective stereoselectors where the difference in *trans* influence between donor atoms differentiates the two binding sites electronically. Furthermore, heterodonor ligands with sp^3 N and/or S donoratoms can form a new stereogenic center upon coordination to the metal and can therefore increase the likelihood of the effective stereochemical communication between the catalyst and the substrate. It is therefore not surprising that the application of these systems in iridium-catalyzed asymmetric hydrogenation and transfer hydrogenation [9], palladium-catalyzed allylic substitution [10], or in copper-catalyzed diethyl zinc addition [11] represents a powerful tool for the synthesis of enantiomerically enriched chiral compounds. In a view of these, it is rather surprising that there is no comprehensive study available on the ring size effects of directly analogous heterodonor ligands with stereolabile coordinating functionalities neither in catalysis nor in coordination chemistry.

Recently, we have developed new chiral P,N [12] and S,N [10e] ligand families based on pentane-2,4-diyl backbone capable of forming six-membered chelate rings. The coordination chemistry and the catalytic behavior of the novel compounds were thoroughly screened as a function of (i) the donoratom (P vs. S), (ii) the substituents of the N or S atoms and (iii) the cooperativity between the stereogenic elements of the backbone. The rationalization of the factors directing the coordination of the ligands and the subsequent stereoelectronic fine-tuning led to very high activities and enantioselectivities (up to 96%) in asymmetric allylic substitution reactions.

In order to gain a deeper insight into the coordination chemistry and catalytic applications of simple chiral alkane-diyl based heterodonor ligands we decided to broaden the scope of our ligand library and developed the synthesis of new ligands with stereolabile donoratom(s) and different tether length to form five- and seven-membered chelates. Our primary aim was to vary the conformational rigidity and the bite angle of the chelate rings by changing the tether length of the ligands. In the present paper we intend to discuss in detail the coordination and catalytic features of directly analogous heterodonor ligands capable of forming five-, six- and seven-membered chelate rings.

2. Synthesis of the new ligands

In our previous reports, it has been shown that pentane-2,4-diyl based heterobidentate P,N and S,N ligands can readily be synthesized via nucleophilic ring opening of optically active cyclic sulfate esters [10e,12b]. The easily available starting materials, the straightforward synthesis, the high yields and stereoselectivities prompted us to prepare P,N and S,N ligands with butane-2,3-diyl and hexane-2,5-diyl backbone in a similar manner. Thus, the analogous optically pure cyclic sulfates of (*S,S*)-butane-2,3-diol (**1**, Scheme 1) and (*S,S*)-hexane-2,5-diol (**4**, Scheme 3) were used as starting materials.

At first, zwitterionic sulfated amines **2** and **3** were synthesized in the nucleophilic ring opening of cyclic sulfate **1** with Me_2NH and $iPrNH_2$, respectively (Scheme 1). The reaction proceeded smoothly, under ambient temperature in THF with complete inversion at the stereogenic center. It was unambiguously proved by NMR, since compounds **2** and **3** exhibited only one signal set in their ^1H NMR spectra indicating the absence of other diastereomeric species. In the next step, the addition of an excess of $LiPPh_2 \cdot$ dioxane to compounds **2** and **3** resulted in the substitution of the $-OSO_3^-$ group. Interestingly, the reaction of compound **2** provided a mixture of two diastereomeric aminoalkyl-phosphines, (*S,R*)-**L1** and (*R,R*)-**L1**. Fortunately, compounds (*S,R*)-**L1** and (*R,R*)-**L1** could readily be separated by column chromatography and characterized separately in their pure form. The absolute configuration of the carbon stereocenters in the ligands was unequivocally determined by the X-ray and NMR analysis of their Pd(II)-complexes.

The formation of the diastereomers can be explained by the presence of two competitive reaction pathways. First, the S_N2 displacement of the sulfate group from **2** by the diphenylphosphide anion provides the product with (*R,R*) stereochemistry. Second, in the presence of $LiPPh_2$ as a base, an intramolecular nucleophilic substitution can also take place with complete inversion at the stereogenic center yielding the corresponding quaternary aziridinium ion (Scheme 2) [13]. The nucleophilic attack of the diphenylphosphide anion at either carbon stereocenter of the three-membered heterocycle results in the formation of the aminoalkyl-phosphine with (*S,R*) configuration. Although the reaction conditions applied favor bimolecular nucleophilic mechanisms, the involvement of non-stereospecific pathways cannot be excluded.

Interestingly, the reaction of aminoalkyl sulfate **3** with $LiPPh_2$ resulted in the formation of one single diastereomer as evidenced by NMR spectroscopy. The absolute configuration of (*R,R*)-**L2** was determined by the analysis of the X-ray structure of its Pd(II) complex (Fig. 2). It is important to note that the reaction of pentane-2,4-diyl based aminoalkyl sulfates with $LiPPh_2$ leads to the formation of a single homochiral diastereomer regardless of the structure of amine functionality. These observations nicely demonstrate that the length of the backbone and substitution pattern of the amine moiety strongly influence the stereochemical outcome of this synthetic methodology. Furthermore, in view of these, it is not surprising that the ring opening of cyclic sulfate **4** with *iso*propylamine and the subsequent reaction with lithium-diphenylphosphide results in the stereoselective formation of ligand (*R,R*)-**L3** (Scheme 3).

The butane-2,3-diyl based ligand (*S,R*)-**L4** was also synthesized starting from compound **3**. In this case the acidic hydrolysis of the sulfate was followed by the substitution of the OH-group according to the Hata-procedure (Scheme 4) [14]. The product formed as a single diastereomer with (*S,R*) configuration at the carbon centers according to its ^1H and ^{13}C NMR spectra and the X-ray (Fig. 2) and NMR analysis of the complex [Pd(**L4**)Cl_2]. These observations imply that compound (*S,R*)-**L4** can be produced stereoselectively with a heterochiral carbon backbone.

The acidic hydrolysis of **3** to **6** occurs with the retention of configuration as indicated by the ^1H NMR data of compound **6** as a single diastereomer. The high stereoselectivity of the next step starting from the aminoalcohol, can be explained by the formation of a homochiral aziridinium intermediate, whose subsequent ring opening with the nucleophilic agent leads to compound (*S,R*)-**L4** (Scheme 5).

In order to compare the backbone substituent effects of the ligands in coordination chemistry and catalysis we have synthesized chiral compounds (*R*)-**L5** and (*S*)-**L6** with only one stereogenic element in their backbone adjacent to the S and N atoms, respectively, and the achiral ligand **L7**. Compound (*R*)-**L5** was prepared in three steps from commercially available ethyl-(*S*)-lactate. The synthesis of the amide **7** was followed by the substitution of the hydroxyl group that occurs with inversion of the configuration at the carbon center [10e]. The subsequent reduction of amide **8** with THF-borane adduct produces the product (*R*)-**L5** (Scheme 6).

Ligand (*S*)-**L6** was synthesized from commercially available (*S*)-alaninol using the Hata protocol and the subsequent alkylation of the corresponding primary amine **7** (Scheme 7). The synthesis of the achiral ligand **L7** was accomplished in one single Hata-reaction step. (Scheme 7).

Compound (*R,R*)-**L8** having hexane-2,5-diyl backbone was prepared stereoselectively similarly to its pentane-2,4-diyl based analogues, starting from aminosulfate **5** as it was revealed by its ^1H

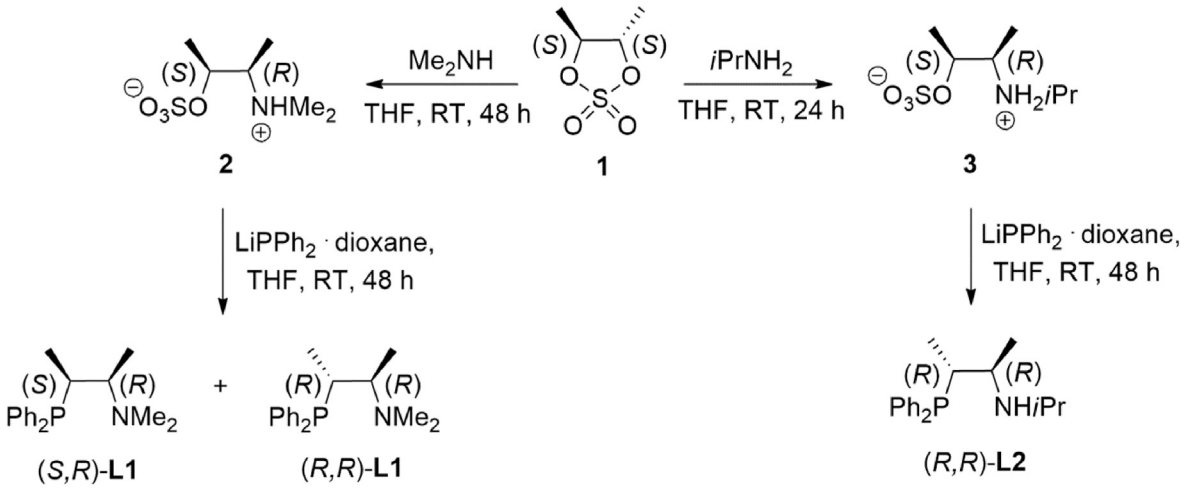

Scheme 1. Synthesis of chiral ligands (*S,R*)- and (*R,R*)-**L1** and (*R,R*)-**L2** starting from cyclic sulfate **1**.

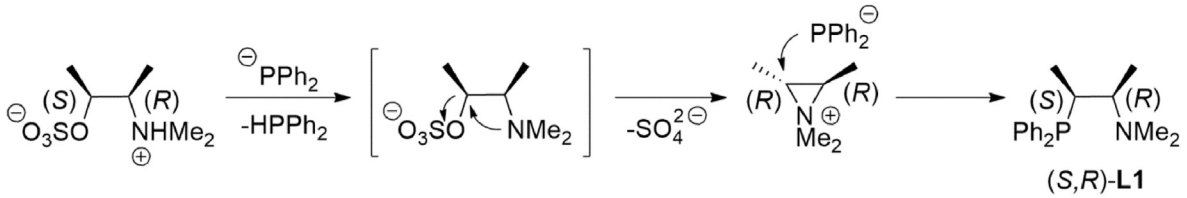

Scheme 2. Sequential double displacement leading to ligand (*S,R*)-**L1**.

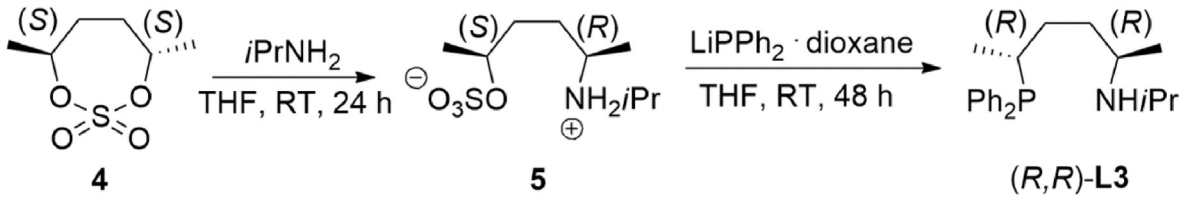

Scheme 3. Synthesis of ligand (*R,R*)-**L3**.

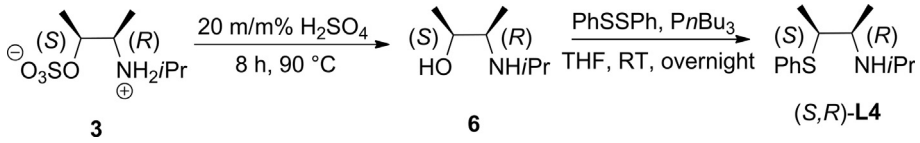

Scheme 4. Synthesis of ligand (*S,R*)-**L4** starting from the corresponding aminoalkyl sulfate **3**.

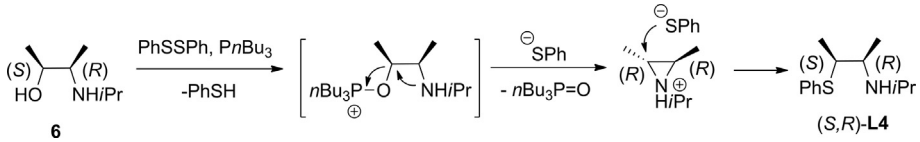

Scheme 5. Proposed mechanism for the stereoselective formation of ligand (*S,R*)-**L4**.

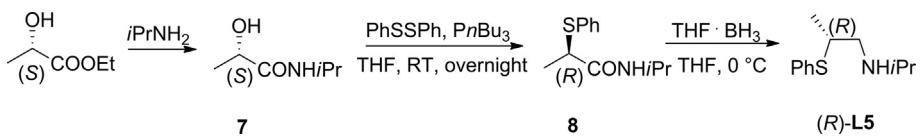

Scheme 6. Multistep synthesis of (*R*)-**L5**.

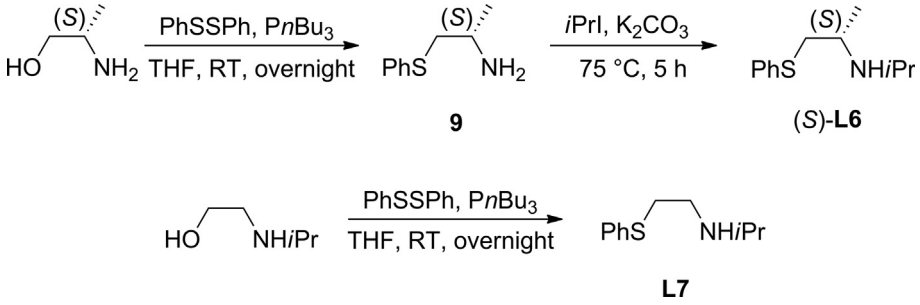

Scheme 7. Synthesis of ligands (*S*)-**L6** and **L7**.

and ^{13}C NMR spectrum (Scheme 8).

3. Synthesis of complexes [Pd(L1-L7)Cl$_2$]

The treatment of [Pd(COD)Cl$_2$] with the solution of 1 molar equivalent of ligands **L1-L7** resulted in the formation of [Pd(**L1-L7**)Cl$_2$] type complexes as yellow solids in good yields. The complexes were characterized by elemental analysis as well as by ^{1}H, $^{13}C\{^{1}H\}$ and $^{31}P\{^{1}H\}$ NMR spectroscopy.

4. X-ray studies on palladium complexes

The objectives of the crystal structure analysis of complexes [Pd((*S*,*R*)-**L1**)Cl$_2$], [Pd((*R*,*R*)-**L2**)Cl$_2$] and [Pd((*S*,*R*)-**L4**)Cl$_2$] were to determine the absolute configuration of the carbon stereocenters in the corresponding ligands and to assess coordination chemistry with special attention to the conformation of the five-membered ring and the configuration of the stereolabile (S or N) donoratoms.

Single crystals suitable for X-ray analysis were grown by slow evaporation of the solvent from the solutions of [Pd((*S*,*R*)-**L1**)Cl$_2$], [Pd((*R*,*R*)-**L2**)Cl$_2$] and [Pd((*S*,*R*)-**L4**)Cl$_2$] in acetone or dichloromethane. In each case the ligand coordinated in a bidentate fashion to form five-membered chelates. It is generally accepted that the five-membered chelate ring can adopt half chair (skew), envelope or distorted envelope conformations as depicted in Fig. 1 [15].

Complex [Pd((*S*,*R*)-**L1**)Cl$_2$] with one independent structure in the unit cell is stabilized in a δ-envelope-like conformation. By definition [15], in the envelop conformation the corresponding endocyclic torsion angles (N−Pd−P-C$_{ring}$ and P−Pd−N-C$_{ring}$ in the case of [Pd((*S*,*R*)-**L1**)Cl$_2$]) are quite different in magnitude but have the same sign, thus exhibiting a "steep" (the torsion is large) and "flat" side (the torsion is small) of the complex. Indeed, in [Pd((*S*,*R*)-**L1**)Cl$_2$] the torsion angles N−Pd−P-C$_{ring}$ (6.6(1)°) and P−Pd−N-C$_{ring}$ (21.5(2)°) are responsible for the presence of a flattened P-side and a puckered N-side (Fig. 2, Table 1). The methyl-substituents on the carbon backbone are positioned equatorially and axially moving from the phosphorus towards the nitrogen, respectively. In the δ-envelope conformation, the absolute values of the two P−Pd−N−C$_{Me}$ torsion angles on the "steep" side of the chelate are quite different (144.2(3)° vs. 99.3(2)°) in contrast to the two N−Pd-X-C$_{Ph,ipso}$ torsions (122.7(1)° vs. 114.7(1)°) that are measured on the "flat" side. This clearly indicates that the two N-methyl groups can straightforwardly be considered as axial (having the higher P−Pd−N−C$_{Me}$ torsion) and equatorial (having the lower P−Pd−N−C$_{Me}$ torsion angle) substituents. As the steric differentiation between the two P-phenyls are much less pronounced, these substituents on the in-plane P atom are best described as inclinal.

Interestingly, in the unit cell of [Pd((*R*,*R*)-**L2**)Cl$_2$] two independent molecules were found with different nitrogen configuration ([Pd((*R*,*R*,*R*$_N$)-**L2**)Cl$_2$] and [Pd((*R*,*R*,*S*$_N$)-**L2**)Cl$_2$]). In complex [Pd((*R*,*R*,*R*$_N$)-**L2**)Cl$_2$] the distorted envelope chelate ring adopts a λ-conformation with equatorially directed methyl-substituents. The nitrogen substituents, H and *i*Pr on the "steep" side of the chelate, can clearly be denoted as equatorial and axial based on the torsion angles P−Pd−N−H = −144.6° and P−Pd−N-C$_{iPr}$ = 101.3(5)°, respectively. Although the difference in the displacement of the P-phenyls with respect to N−Pd−P plane is larger (absolute values of the torsion angles N−Pd-X-C$_{Ph,ipso}$ = 124.9(3)° vs. 108.5(3)°) than in complex [Pd((*S*,*R*)-**L1**)Cl$_2$], their equatorial and axial positions are still hardly distinguishable. Contrarily, in [Pd((*R*,*R*,*S*$_N$)-**L2**)Cl$_2$], P-phenyl rings are clearly equatorial (N−Pd-X-C$_{Ph,ipso}$ = −139.9(4)°) and axial (N−Pd-X-C$_{Ph,ipso}$ = 93.2(3)°). In exchange, the spatial orientation of the N-substituents becomes quite similar (P−Pd−N−H = 118.4° and P−Pd−N-C$_{iPr}$ = −128.8(6)°) in this case. Although [Pd((*R*,*R*,*S*$_N$)-**L2**)Cl$_2$] is also stabilized in a λ-conformation, the steep and flat sides interchange due to the variation of the endocyclic torsion angles. This is possibly due to the inversion of the nitrogen configuration.

Finally, compound [Pd((*S*,*R*)-**L4**)Cl$_2$] also exhibited two independent molecules in the asymmetric unit, that form envelop and distorted envelop conformations, respectively. In both cases, the five-membered chelate is stabilized in a δ-conformation, with equatorially and axially positioned methyl-substituents, moving from the sulfur towards the nitrogen. Similarly to [Pd((*S*,*R*)-**L1**)Cl$_2$], the steep side of the complexes is around the nitrogen (S−Pd−N-C$_{ring}$: 37.7(4) and 28.2(3)°, respectively) and the flat side is around the sulfur (N−Pd−S-C$_{ring}$ = -8.8(3) and 1.8(2)°, respectively). Consequently, the N−H is clearly equatorial and the N-*i*Pr is clearly

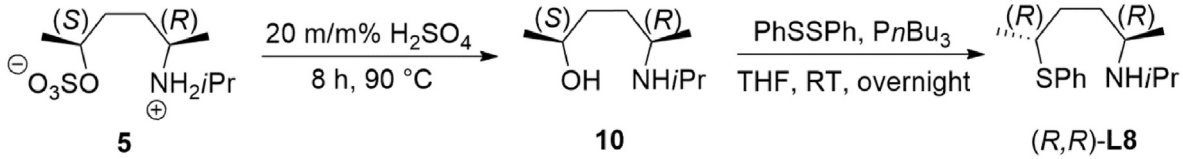

Scheme 8. Synthesis of ligand (*R*,*R*)-**L8**.

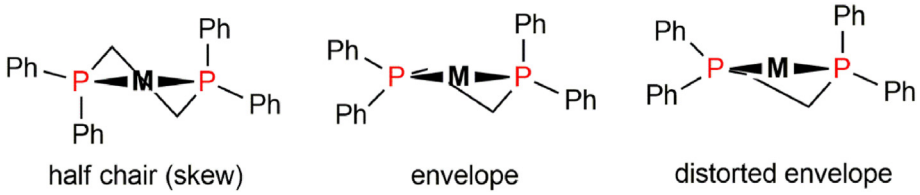

Fig. 1. Conformations of five-membered chelates. λ-skew (half chair), envelope and distorted envelope conformation of dppe metal-chelates.

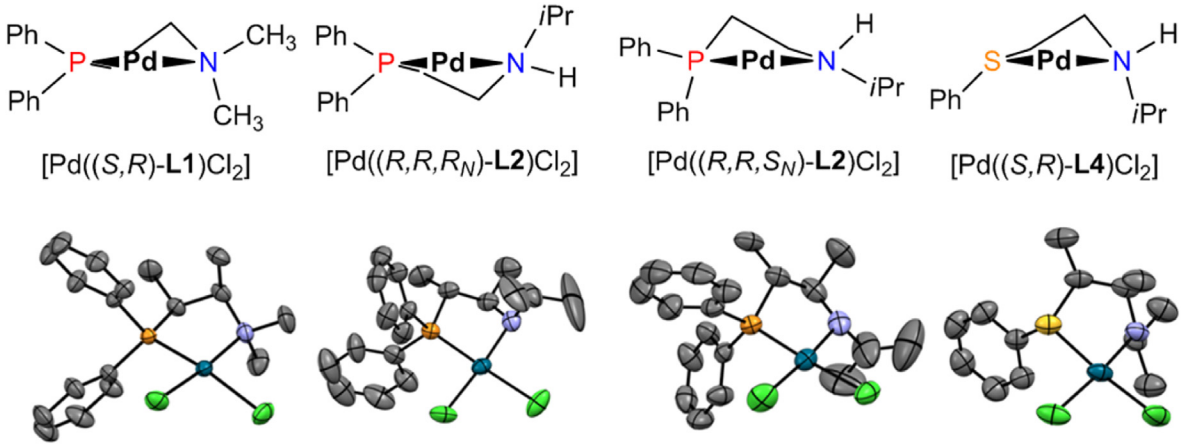

Fig. 2. Schematic and ORTEP views of five-membered chelates. (In schematic views the backbone methyl substituents and in the ORTEP views the hydrogens are omitted for clarity. The ORTEP views are depicted at 30% probability level.)

Table 1
Selected bond lengths (Å), bond angles (°) and torsion angles (°).

	[Pd((*S*,*R*)-**L1**)Cl$_2$]	[Pd((*R*,*R*,*R*$_N$)-**L2**)Cl$_2$]	[Pd((*R*,*R*,*S*$_N$)-**L2**)Cl$_2$]		[Pd((*S*,*R*)-**L4**)Cl$_2$]
ring conformation	envelope	dist. env.	dist. env.	dist. env.	envelope
Pd-X (X = P or S)	2.2925(9)	2.198(2)	2.1766	2.266(2)	2.254(2)
Pd−N	2.109(3)	2.076(6)	2.1196	2.069(7)	2.081(5)
Pd−Cl (*trans* to X)	2.378(1)	2.380(2)	2.3926	2.315(2)	2.323(2)
Pd−Cl (*trans* to N)	2.2925(9)	2.298(2)	2.2975	2.296(2)	2.299(2)
X-Pd-N	86.89(8)	85.1(2)	84.56	85.7(2)	87.0(1)
Cl−Pd−Cl	91.87(4)	93.04(8)	91.45	92.3(1)	92.20(7)
X-Pd-N-C$_{ring}$	21.5(2)	−32.9(4)	4.0(4)	37.7(4)	28.2(3)
N−Pd-X-C$_{ring}$	6.6(1)	7.8(3)	−26.4(3)	−8.8(3)	1.8(2)
X-Pd-N-Y^1 (Y^1 = C of CH$_3$ or H)	144.2(3)	−144.6	118.4	153(6)	146(4)
X-Pd-N-Y^2 (Y^2 = C of CH$_3$ or methine C of *i*Pr)	−99.3(2)	101.3(5)	−128.8(6)	−91.2(5)	−100.0(4)
N−Pd-X-C(Ph^1)$_{ipso}$	−114.7(1)	−108.5(3)	−139.9(4)	98.3(3)	109.6(3)
N−Pd-X-C(Ph^2)$_{ipso}$	122.7(1)	124.9(3)	93.2(3)	–	–
Pd-X-C(Ph^1)$_{ipso}$-C(Ph^1)$_{ortho}$	3.4(3)	−44.3(6)	42.1(8)	−3.3(8)	−26.4(8)
Pd-X-C(Ph^2)$_{ipso}$-C(Ph^2)$_{ortho}$	88.0(3)	−34.8(8)	39.1(6)	–	–

axial. The configurations of the stereolabile donoratoms in both conformations of [Pd((*S*,*R*)-**L4**)Cl$_2$] are (*S*$_S$, *S*$_N$).

5. Solution phase NMR studies

In order to gain a deeper insight into the solution phase structure of complexes [Pd(**L1**-**L7**)Cl$_2$], they were investigated by ^{1}H, ^{13}C{^{1}H} and ^{31}P{^{1}H} NMR methods and in several cases by ^{1}H−^{1}H COSY, ^{1}H−^{1}H NOESY and ^{1}H−^{13}C HSQC techniques using CD_2Cl_2 as solvent.

According to the simple ^{1}H, ^{13}C{^{1}H} and ^{31}P{^{1}H} NMR spectroscopy, complexes [Pd((*S*,*R*)-**L1**)Cl$_2$] and [Pd((*R*,*R*)-**L1**)Cl$_2$] exist as single diastereomers in their solutions. The ^{1}H NMR spectrum of [Pd((*S*,*R*)-**L1**)Cl$_2$] exhibited large *trans* coupling between the phosphorus and the CH(N) methine ($^3J(^{31}P,^1H)$ = 38.4 Hz) and a relatively small coupling ($^3J(^1H,^1H)$ = ~5 Hz) between the two methine protons of the backbone could be observed (Fig. 3). Additionally, according to the ^{13}C{^{1}H} spectrum the coupling constant between the phosphorus and the backbone methyl carbon adjacent to the nitrogen is remarkably small ($^3J(^{31}P,^{13}C)$ = ~5 Hz). Based on the Karplus relation, these coupling constants suggests that the backbone methyl substituents are arranged equatorially and axially, moving from the phosphorus towards the nitrogen, respectively [16]. Consequently, the conformation of the complex is similar to that found in the crystal (Fig. 2). As expected, the analysis of the corresponding coupling constants of [Pd((*R*,*R*)-**L1**)Cl$_2$] ($^3J(^{31}P,^1H)$ = 10.2 Hz, $^3J(^1H,^1H)$ = 12.8 Hz, $^3J(^{31}P,^{13}C)$ = 18.8 Hz) proves that the two methyl groups are equatorially positioned (Fig. 3).

The NMR spectra of complex [Pd((*R*,*R*)-**L2**)Cl$_2$**]** exhibited two signal sets indicating the presence of two isomer complexes in solution. In this case the ^{13}C{^{1}H} spectrum proved to be very

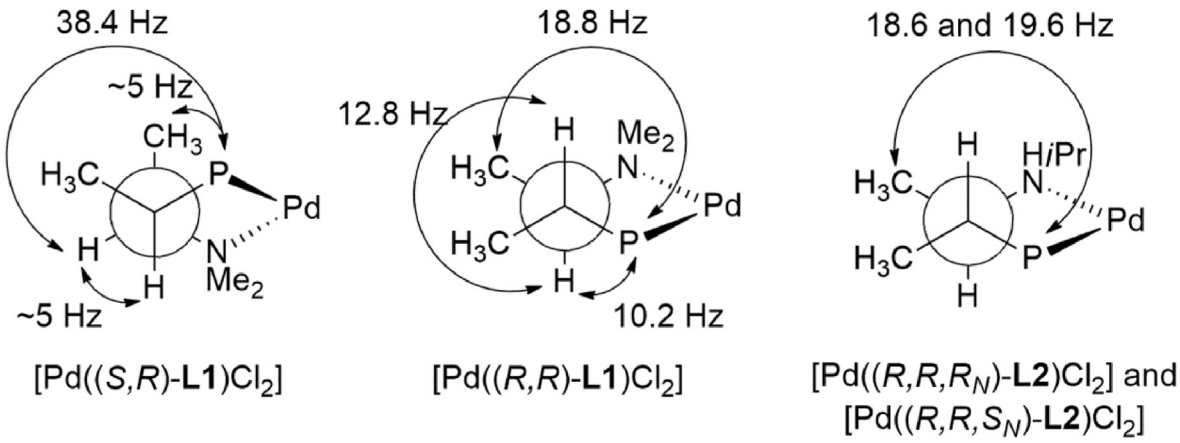

Fig. 3. Ring conformations of complexes [Pd((*S*,*R*)-**L1**)Cl_2], [Pd((*R*,*R*)-**L1**)Cl_2], [Pd((*R*,*R*,R_N)-**L2**)Cl_2] and [Pd((*R*,*R*,S_N)-**L2**)Cl_2] in solution. (The coupling constants were measured at room temperature using CD_2Cl_2 as solvent. The P-Ph substituents are omitted for clarity.)

informative concerning the conformation of the two species. Both diastereomers exhibit large $^3J(^{31}P,^{13}C)$ couplings (19.6 and 18.6 Hz) between the phosphorus and backbone methyl carbon on the N-side, indicating the equatorial position of this methyl substituent (Fig. 3) [16]. As the ligand has (*R*,*R*) backbone chirality the position of the other methyl group is also equatorial in both species. It is therefore reasonable to assume that the [Pd((*R*,*R*,R_N)-**L2**)Cl_2] and [Pd((*R*,*R*,S_N)-**L2**)Cl_2] isomers found in the solid phase are present in the solution.

Complex [Pd((*R*,*R*)-**L3**)Cl_2] having four carbon atoms between its coordinating functionalities revealed seven broad signals in its ^{31}P NMR spectrum between 36.34 and 34.93 ppm at room temperature in $CDCl_3$, suggesting the presence of several species in dynamic equilibrium. These could arise from the different conformations of chelate species or from multinuclear complexes [17]. As the resonances of phosphorus in the $^{31}P\{^1H\}$ spectrum as well as the ^1H NMR signals of the N-methyl protons in the major components are remarkably shifted with respect to the free ligand, it is reasonable to assume that both the N- and P-atoms are involved in coordination.

Surprisingly, complex [Pd((*S*,*R*)-**L4**)Cl_2] exists in solution as a single isomer. Upon cooling the sample to 193 K, the ^1H spectrum still exhibited only one signal set indicating the absence of fast equilibria between different stereoisomers. The relatively small coupling between its backbone methine protons ($^3J(H,H) = 4.4$ Hz) proves that the methyl substituents are equatorially and axially arranged similarly to [Pd((*S*,*R*)-**L1**)Cl_2] (Fig. 3). According to these, it might be concluded that complex [Pd((*S*,*R*)-**L4**)Cl_2] is stabilized in the same conformer in solution as in the solid phase (Fig. 2).

Complex [Pd((*R*)-**L5**)Cl_2] with one chiral center in the backbone is present in solution as a mixture of two diastereomers in a ratio of 0.65:1. As the coupling patterns of the two diastereotopic methylene protons in the backbone are essentially the same for the two isomers, it is reasonable to assume that they have the same ring conformation. Thus, they must differ in the configuration of their donoratom(s). Furthermore, the coupling constants of the two methylene hydrogens to the adjacent methine differ significantly ($^3J(^1H,^1H) = 12.8$ Hz and 3.9 Hz) that is only possible in structure having an equatorial Me-subtituent. Likewise, [Pd((*S*)-**L6**)Cl_2] can be found in CD_2Cl_2 as a diastereomeric mixture. In this case, however, only one broad signal set can be observed in the ^1H and $^{13}C\{^1H\}$ NMR spectra at room temperature. Upon cooling the sample to 253 K three isomers appears in the ^1H spectrum in a molar ratio of 1:2.4:11. Based on the considerations detailed for [Pd((*R*)-**L5**)Cl_2] the backbone methyl substituent of [Pd((*S*)-**L6**)Cl_2] is also positioned equatorially in the major isomer. Unfortunately, for the two minor complexes no accurate analysis could be performed due to their lower concentration and the overlapping of the corresponding NMR signals. Finally, complex [Pd(**L7**)Cl_2] exhibited a simple ^1H NMR spectrum containing only one set of signals. As it was expected, a fast ring inversion takes place that is possibly coupled with donoratom inversion.

According to the solid phase X-ray and solution phase NMR studies it can nicely be deduced that the chiral backbone in the five-membered palladium(II) chelates is able to efficiently control the ring conformation. In each case the chelate ring is stabilized in a single conformation in solution. Consequently, when more than one isomer appears in solution (eg. in the case of [Pd((*R*,*R*,R_N)-**L2**)Cl_2], [Pd((*R*,*R*,S_N)-**L2**)Cl_2], [Pd((*R*)-**L5**)Cl_2] and [Pd((*S*)-**L6**))Cl_2], they must differ in their donoratom configuration(s).

6. Catalytic properties and discussion

In order to compare the catalytic performance of the chiral ligands capable of forming chelate rings of different size, they were tested in palladium-catalyzed asymmetric allylic alkylation reaction that is one of the most versatile methods for asymmetric C—C bond-forming processes. Furthermore, as the elementary steps of the catalytic cycle are well understood, the stereochemical outcome of the reaction might provide valuable information on fundamental substrate-ligand interactions. In this context (i) the conformational flexibility of the chelate ring, (ii) the configurational stability of the donoratoms, (iii) the stereoselectivity of the substrate's coordination and (iv) the stereoelectronic differentiation of the diastereotopic allylic termini are crucial in determining the enantioselectivity of the reaction.

Ligands **L1-L8** were studied in the Pd-catalyzed asymmetric allylic alkylation of the benchmark substrate diphenylallyl acetate with dimethyl malonate in the presence of KOAc/BSA as base (Table 2). The catalytic reactions were performed in CH_2Cl_2 as solvent at a substrate/catalyst molar ratio of 100 and were followed by TLC. Generally, catalysts containing S,N-ligands (entries 5—10) required a prolonged reaction time (48 h) to proceed compared to the Pd-complexes modified by phosphine-amines (entries 1—4) that provided the product with full conversion within 1 h. Interestingly, the activity of the reaction was also strongly affected by the substitution pattern of the ligands' backbone. It is most obvious from the conversions achieved with S,N ligands **L4-L7** (entries 5—8). In these cases the backbone methyl substituents can not only sterically affect the structure of the catalytically active species but

Table 2
Asymmetric allylic alkylation of diphenylallyl acetate with the Pd-complexes of several heterobidentate ligands.[a]

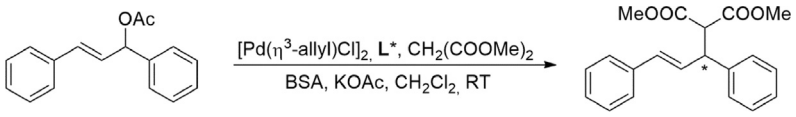

Entry	Ligand	Ligand's structure	Reaction time (h)	Conversion (%)	*Ee* (%)
1	(*S*,*R*)-**L1**	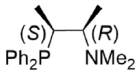	1	>99	38 (*R*)
2	(*R*,*R*)-**L1**	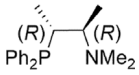	1	>99	72 (*S*)
3	(*R*,*R*)-**L2**	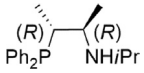	1	>99	44 (*S*)
4	(*R*,*R*)-**L3**	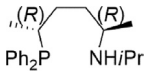	1	>99	4 (*S*)
5	(*S*,*R*)-**L4**	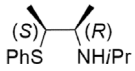	48	31	87 (*S*)
6	(*R*)-**L5**	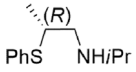	48	>99	12 (*R*)
7	(*S*)-**L6**	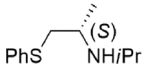	48	5	67 (*R*)
8	**L7**	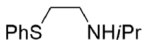	48	54	–
9	(*R*,*R*)-**L8**	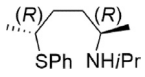	48	0	–
10[b]	(*S*,*S*)-**L9**	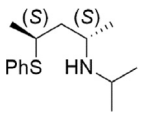	48	>99	90 (*R*)
11[c]	(*S*,*S*)-**L10**	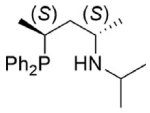	1	>99	94 (*R*)

[a]Reaction conditions: catalyst prepared *in situ* from 0.5 mol% of $[(\eta^3\text{-}C_3H_5)PdCl]_2$ and 1 mol% of chiral ligand; substrate 1.25 mmol; dimethyl malonate 3.75 mmol; solvent 10 mL of CH_2Cl_2; BSA 3.75 mmol; KOAc 7 mg; temperature RT. Conversion and enantiomeric excess were determined by chiral HPLC. [b]See ref. 10e. [c]See ref. 6a.

the electronic properties of the donoratoms may also be strongly influenced.

Table 2 also presents the catalytic results achieved in our previous studies with six-membered chelating ligands (*S*,*S*)-**L9** [10e] and (*S*,*S*)-**L10** [6a] (entries 10 and 11). The data obtained by the homologous five-, six- and seven-membered homochiral P,N-ligands (*R*,*R*)-**L2**, (*R*,*R*)-**L3** and (*S*,*S*)-**L10**, respectively, clearly indicate that the best enantioselectivity (94%) can be achieved by the six-membered chelate. According to the NMR studies of the dichloro complexes [Pd((*R*,*R*)-**L2**)Cl_2] and [Pd((*R*,*R*)-**L3**)Cl_2], it is reasonable to assume that the major factor responsible for the decreased enantioselectivity of the catalysts modified by (*R*,*R*)-**L2** and (*R*,*R*)-**L3** is the non-stereoselective coordination of the ligands. In contrast, ligand (*S*,*S*)-**L10** is able to stereoselectively coordinate to Pd to form one single six-membered chelate isomer. Possibly, in the case of ligands (*R*)-**L5** and (*S*)-**L6** the same phenomenon is responsible for the reduced enantioselectivity compared to (*S*,*R*)-**L4**. As it was noticed earlier, in five-membered chelates [Pd((*R*,*R*)-**L2**)Cl_2], [Pd((*R*)-**L5**)Cl_2] and [Pd((*S*)-**L6**)Cl_2] the difference between the various isomers present in their solutions is the configuration of their donoratoms. In five-membered chelates, however, the ring conformation is less prone to change compared to their six-membered analogues, where the ring inversion has also been identified as a source of diastereoisomerism [6a]. It is therefore not surprising that in seven-membered chelates the pronounced flexibility of the ring might significantly increase the number of conformers.

Moreover, it is also apparent that in five-membered systems the stereocontrol of the *cis* co-ligands (eg. Cl) on the donoratom configuration is less pronounced that is due to the decreased bite angle of the chelates resulting in reduced interligand interactions (Fig. 4). It also necessitates the reduced control on the donoratom configuration. Accordingly, based on the wider bite angle of seven-membered chelates [18] one could expect more stereocontrol on

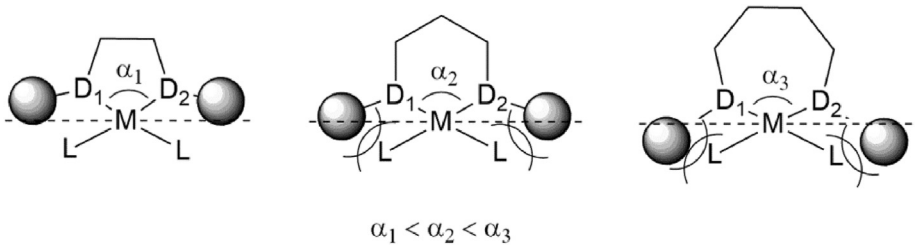

Fig. 4. Effect of bite angle on interligand interactions.

donoratom coordination. However, in this case the high conformational flexibility of the ring strongly reduces the stereoselectivity of donoratom coordination. Furthermore, in these cases the possibility of the formation of multinuclear species is remarkably increased to the longer tether and the hemilability of the ligands.

As an additional consequence of the weaker interligand interactions in five-membered systems it is surmised that the stereoselectivity of the substrate coordination is also lower. Furthermore, the regioselectivity of the nucleophilic attack in allylic alkylation reactions is also strongly depends on the bite angle of the ligand [19]. It is in line with the observation that the enantioselectivities provided by five-membered chelating ligands (*S,R*)-**L1**, (*R,R*)-**L1** and (*S,R*)-***L4*** (entries 1, 2 and 5) capable of stereoselective coordination are smaller than those achieved by their six-membered analogues ((*S,S*)-**L9** and (*S,S*)-**L10**). Although, these five-membered systems are not directly analogous to (*S,S*)-**L9** and (*S,S*)-L**10**, it is reasonable to assume that the differences in their catalytic properties are mainly attributable to their different bite angles and substrate-ligand interactions.

7. Concluding remarks

A series of novel chiral heterodonor P,N and S,N ligands capable of forming five- and seven-membered chelate rings has been synthesized. The new compounds were prepared by the ring opening of cyclic sulfate esters or by using naturally occurring chiral compounds. It was shown that the synthesis of butane-2,3-diyl based ligands starting from the corresponding cyclic sulfate can proceed through aziridinium intermediates resulting in the formation of various stereoisomers. Based on our combined X-ray, NMR and catalytic studies the following conclusions can be drawn concerning the palladium coordination chemistry of the new chiral heterodonor ligands capable of forming chelate rings of different size. (i) The conformational rigidity of the chelate ring increases with the decreasing ring size; in the case of the five-membered ring complexes, only one chelate conformer could be found in solution by NMR. (ii) The configuration of the stereogenic donoratoms can more effectively be regulated in chelate rings with wider bite angle due to the more expressed steric interaction between the donoratom substituents and the *cis* co-ligand. The conformation of the chelate ring, however, might strongly affect the stereoselectivity of the donoratom coordination. (iii) The narrower the bite angle leads to weaker substrate ligand interactions that might have a detrimental effect on the stereoselectivity of the substrate coordination and hence on the *ee* of the catalytic reaction. Accordingly, there is a delicate balance between bite angle effects and the stereoselectivity of the coordination. As the six-membered chelate rings can form stereoselectively regarding both the ring conformation and the donoratom configuration and exhibit relatively wide bite angle it is not surprising that they have generally superior catalytic performance in asymmetric allylic substitution reactions compared to their five- or seven-membered analogues. Although, this trend may not hold for other catalytic processes, the fundamental relationships between the ring size of the heterodonor chelates and their coordination chemistry can be utilized in a number of transition metal catalyzed asymmetric transformations.

Declaration of competing interest

The authors declare that they have no known competing financial interests or personal relationships that could have appeared to influence the work reported in this paper.

Acknowledgements

We thank Mr Béla Édes for skillful assistance in analytical measurements and synthetic experiments. The research was supported by the project NKFIH K128074. The research was also supported by the EU and co-financed by the European Regional Development Fund under the projects GINOP-2.3.2-15-2016-00008 and GINOP-2.3.3-15-2016-00004.

Appendix A. Supplementary data

Supplementary data to this article can be found online at https://doi.org/10.1016/j.jorganchem.2020.121332.

8. Experimental

General experimental details. All manipulations were carried out under argon using Schlenk techniques. Solvents were purified, dried and deoxygenated by standard methods. Compounds **2**, (*R,R*)-**L1**, [Pd((*R,R*)-**L1**)Cl_2] [20], **7** [21] and [Pd(COD)Cl_2] [22] were prepared according to literature methods. All other starting materials were purchased from Sigma Aldrich. $^{31}P\{^1H\}$-, $^{13}C\{^1H\}$- and ^1H NMR measurements were carried out on a Bruker Avance 400 spectrometer (NMR Laboratory, University of Pannonia) operating at 161.98, 100.61 and 400.13 MHz respectively. The ^1H NMR and ^{13}C NMR signals were assigned from their related $^1H-^1H$ COSY and $^{13}C-^1H$ HMQC spectra, respectively. In order to facilitate structure elucidation, $^1H-^1H$ NOESY spectra were also recorded. ESI mass spectra were recorded on an Agilent 1100 LC/MSD SL Quadrupole mass spectrometer (Department of Earth and Environmental Science, University of Pannonia). X-ray data were collected on a Bruker-Nonius MACH3 diffractometer. For further details of structure determination by X-ray diffraction see Supplementary Information.

8.1. (2R,3S)-3-(diphenylphosphino)-N,N-dimethylbutan-2-amine ((S,R)-L1)

$LiPPh_2$1,4-dioxane adduct (8.4 g, 30 mmol) was dissolved in THF (30 mL) under argon and the solution was cooled to −10 °C. (2*R*,3*S*)-

2-dimethylamino-3-sulfatobutane (1.2 g, 6 mmol) was added to the red solution in small portions. The reaction mixture was stirred at room temperature for 48 h. The color of the reaction mixture remained red. After evaporation of the solvent, deoxygenated water (60 mL) and ether (40 mL) were added to the residue and the mixture was stirred until the two phases became clear solutions. The pH of the mixture was then adjusted to 1 with 10% deoxygenated HCl solution. The two phases were then separated and the water phase was washed three times with 40 mL portions of ether. The pH was then adjusted to about 9–10 with dropwise addition of a dilute solution of Na_2CO_3. The product was extracted four times with 40 mL portions of ether. After drying with $MgSO_4$ the solvent was evaporated. The crude product mixture was purified by column chromatography (Al_2O_3, eluent: hexane/EtOAc 6/1, Rf: ~0.75) to give (2*R*,3*S*)-3-(diphenylphosphino)-2-dimethylaminobutane ((*S,R*)-**L1**) as a transparent oil. Yield: 0.64 g, 37%. ^{1}H NMR (400 MHz, $CDCl_3$) δ 7.54–7.40 (m, 4H, aromatic), 7.36–7.25 (m, 6H, aromatic), 2.65–2.51 (m, 1H, CH), 2.51–2.39 (m, 1H, CH), 2.25 (s, 6H, $N(CH_3)_2$), 1.10 (d, J = 6.4 Hz, 3H, CH_3), 1.04 (dd, J = 9.3, 7.3 Hz, 3H, CH_3). ^{31}P NMR (162 MHz, $CDCl_3$) δ −3.22 (s). ^{13}C NMR (101 MHz, $CDCl_3$) δ 138.10 (br. s, aromatic, 1C), 136.56 (br. s, aromatic, 1C), 134.91 (d, J = 18.1 Hz, aromatic, 2C), 133.02 (d, J = 18.1 Hz, aromatic, 2C), 129.07 (s, aromatic, 1C), 128.47 (d, J = 6.2 Hz, aromatic, 2C), 128.31 (d, J = 7.3 Hz, aromatic, 2C), 128.30 (s, aromatic, 1C), 61.94 (s, 1C), 41.19 (s, 2C), 35.97 (s, 1C), 14.28 (s, 1C), 11.09 (s, 1C). EI mass spectrum: m/z 285 $[M]^+$ (calculated 285.16 $[M]^+$).

8.2. (2S,3R)-3-(isopropylamino)-2-sulfatobutane (3)

Isopropylamine (0.546 mL, 6.356 mmol) was added to (4*S*,5*S*)-4,5-dimethyl-1,3,2-dioxathiolane 2,2-dioxide (cyclic sulfate of (*S,S*)-butane-2,3-diol) (0.5 g, 3.286 mmol) and the mixture was stirred for 24 h at room temperature. Next, ether (20 mL) was added to the mixture. The suspension formed was stirred for 30 min and then filtered. The solid was washed two times with ether (5 × 6 mL) and dried with azeotropic destillation using toluene. The residual solvent was evaporated by vacuum to give (2*S*,3*R*)-3-(isopropylamino)-2-sulfatobutane as a white powder. Yield: 538 mg, 78%. ^{1}H NMR (400 MHz, DMSO) δ 7.91 (s, 2H, NH_2^+), 4.53 (qd, J = 6.5, 2.0 Hz, 1H, CH), 3.55–3.45 (m, 1H, C*H*$(CH_3)_2$), 3.36 (qd, J = 6.7, 2.0 Hz, 1H, CH), 1.21 (d, J = 6.6 Hz, 3H, CH_3), 1.19 (d, J = 6.5 Hz, 3H, CH_3), 1.19 (d, J = 6.4 Hz, 3H, CH_3), 1.16 (d, J = 6.8 Hz, 3H, CH_3). ^{13}C NMR (101 MHz, DMSO) δ 70.57 (s, 1C, CH), 54.04 (s, 1C, CH), 47.18 (s, 1C, CH), 18.82 (s, 1C, CH_3), 18.63 (s, 1C, CH_3), 17.07 (s, 1C, CH_3), 10.97 (s, 1C, CH_3).

8.3. (2R,3R)-3-(diphenylphosphino)-N-isopropylbutan-2-amine ((R,R)-L2)

Title compound (*R,R*)-**L2** was synthesized according to the procedure described for compound (*S,R*)-**L1**. Yield: 46%. ^{1}H NMR (400 MHz, $CDCl_3$) δ 7.58–7.49 (m, 4H, aromatic), 7.35–7.25 (m, 6H, aromatic), 2.95–2.84 (m, 1H, CH), 2.83–2.75 (m, 1H, CH), 2.74–2.65 (m, 1H, CH), 1.14 (d, J = 6.5 Hz, 3H, CH_3), 0.97 (d, J = 6.1 Hz, 3H, CH_3), 0.96 (dd, J = 13.7, 7.2 Hz, 3H, CH_3), 0.92 (d, J = 6.3 Hz, 3H, CH_3). ^{13}C NMR (101 MHz, $CDCl_3$) δ 137.13 (d, J = 14.3 Hz, 1C, aromatic), 136.93 (d, J = 14.4 Hz, 1C, aromatic), 133.94 (d, J = 20.4 Hz, 2C, aromatic), 133.64 (d, J = 19.8 Hz, 2C, aromatic), 129.07 (s, 1C, aromatic), 128.99 (s, 1C, aromatic), 128.57 (d, J = 7.3 Hz, 2C, aromatic), 128.43 (d, J = 7.5 Hz, 2C, aromatic), 50.04 (d, J = 17.2 Hz, 1C), 45.22 (s, 1C), 34.30 (d, J = 11.4 Hz, 1C), 22.90 (s, J = 29.4 Hz, 1C), 22.60 (s, 1C), 16.22 (s, 1C), 10.19 (d, J = 17.0 Hz, 1C). ^{31}P NMR (162 MHz, $CDCl_3$) δ −8.27 (s). EI mass spectrum: m/z 299 $[M]^+$ (calculated 299.18 $[M]^+$).

8.4. (2S,5R)-5-(isopropylamino)-2-sulfatohexane (5)

Title compound **5** was synthesized according to the procedure described for compound **3**. Yield: 45%. ^{1}H NMR (400 MHz, DMSO) δ 8.02 (s, 1H), 7.98 (s, 1H), 4.22–4.13 (m, 1H, CH), 3.40–3.31 (m, 1H, CH), 3.28–3.20 (m, 1H, CH), 1.81–1.70 (m, 1H, diast. C*H*H), 1.55–1.45 (m, 3H, CH_2), 1.22 (d, J = 6.5 Hz, 3H, CH_3), 1.20 (d, J = 6.4 Hz, 3H, CH_3), 1.16 (d, J = 6.3 Hz, 6H, CH_3). ^{13}C NMR (101 MHz, DMSO) δ 71.33 (s, 1C, CH), 50.08 (s, 1C, CH), 46.46 (s, 1C, CH), 31.99 (s, 1C, CH_2), 28.46 (s, 1C, CH_2), 21.10 (s, 1C, CH_3), 19.21 (s, 1C, CH_3), 18.36 (s, 1C, CH_3), 15.69 (s, 1C, CH_3).

8.5. (2R,5R)-5-(diphenylphosphino)-N-isopropylhexane-2-amine ((R,R)-L3)

Title compound (*R,R*)-**L3** was synthesized according to the procedure described for compound (*S,R*)-**L1**. Yield: 80%. ^{1}H NMR (400 MHz, $CDCl_3$) δ 7.58–7.42 (m, 4H, aromatic), 7.40–7.28 (m, 6H, aromatic), 2.99–2.82 (m, 1H, CH), 2.74–2.58 (m, 1H, CH), 2.40–2.19 (m, 1H, CH), 1.63–1.41 (m, 3H, CH_2), 1.37–1.23 (m, 1H, CH_2), 1.07 (d, J = 5.8 Hz, 3H, CH_3), 1.05 (dd, J = 14.9, 6.9 Hz, 3H, CH_3), 1.03 (d, J = 6.2 Hz, 3H, CH_3), 0.98 (d, J = 6.3 Hz, 3H, CH_3). ^{13}C NMR (101 MHz, $CDCl_3$) δ 136.94 (d, J = 13.9 Hz, 1C, aromatic), 136.76 (d, J = 14.5 Hz, 1C, aromatic), 133.29 (d, J = 19.3 Hz, 2C, aromatic), 132.99 (d, J = 18.9 Hz, 2C, aromatic), 128.25 (s, 1C, aromatic), 128.18 (s, 1C, aromatic), 127.88 (d, J = 7.6 Hz, 2C, aromatic), 127.81 (d, J = 7.7 Hz, 2C, aromatic), 49.52 (s, 1C), 44.97 (s, 1C), 34.29 (d, J = 10.9 Hz, 1C), 29.78 (d, J = 9.4 Hz, 1C), 29.30 (d, J = 17.9 Hz, 1C), 22.82 (s, 1C), 22.27 (s, 1C), 19.75 (s, 1C), 15.74 (d, J = 16.2 Hz, 1C). ^{31}P NMR (162 MHz, $CDCl_3$) δ −1.66 (s). EI mass spectrum: m/z 327 $[M]^+$ (calculated 327.21 $[M]^+$).

8.6. (2S,3R)-3-(isopropylamino)butan-2-ol (6)

A solution of sulfuric acid (45 mL, 20 m/m%) was added to **3** (1 g, 4.74 mmol) and the mixture was stirred for 8 h at 90 °C. The solution was then allowed to cool to room temperature and its pH value was ajdusted to 12 by the addition of Na_2CO_3. The aqueous solution was then extracted with ether (3 × 40 mL) and the combined organic phases were dried with $MgSO_4$. The solvent was evaporated in vacuo to give the title compound as a dense oil. Yield: 415 mg, 66%. ^{1}H NMR (400 MHz, $CDCl_3$) δ 3.72 (qdd, J = 6.5, 3.4, 1.1 Hz, 1H, CH), 2.94–2.83 (m, 1H, CH), 2.73 (qdd, J = 6.6, 3.3, 1.1 Hz, 1H, CH), 1.06 (dd, J = 6.3, 0.9 Hz, 3H, CH_3), 1.04 (dd, J = 6.5, 0.7 Hz, 3H, CH_3), 1.02 (dd, J = 6.3, 0.8 Hz, 3H, CH_3), 0.96 (dd, J = 6.6, 0.9 Hz, 3H, CH_3). ^{13}C NMR (101 MHz, $CDCl_3$) δ 67.38 (s, 1C, CH), 54.47 (s, 1C, CH), 45.90 (s, 1C, CH), 23.39 (s, 1C, CH_3), 23.21 (s, 1C, CH_3), 17.81 (s, 1C, CH_3), 14.54 (s). EI mass spectrum: m/z 131 $[M]^+$ (calculated 131.13 $[M]^+$).

8.7. (2R,3S)–N-isopropyl-3-(phenylthio)butan-2-amine ((S,R)-L4)

To a solution of **6** (200 mg, 1.53 mmol) in THF (0.8 mL), diphenyl disulfide (665 mg, 3.05 mmol) and tri-*n*-butylphosphine (616 mg, 3.05 mmol, 749 μL) were added and the reaction mixture was stirred overnight at RT. The solvent was then evaporated, 5 mL of water was added and the pH was adjusted to 2 by using dilute HCl solution. The mixture was extracted with ether (20 mL) and the pH of the aqueous phase was adjusted to 12 with Na_2CO_3. The alkaline solution was then extracted with ether (4 × 20 mL) and the solvent was evaporated in vacuo. To remove the phosphine oxide byproduct the crude mixture was passed through a short pad of activated Al_2O_3 column by using ether as eluent. The evaporation of the solvent gave the pure product as an oil. Yield: 218 mg, 64%. ^{1}H NMR (400 MHz, $CDCl_3$) δ 7.49–7.39 (m, 2H, aromatic), 7.34–7.27 (m, 2H,

aromatic), 7.26–7.18 (m, 1H, aromatic), 3.46 (m, 1H, CH), 2.96 (m, 1H, CH), 2.93–2.82 (m, 1H, CH), 1.34 (d, $J = 7.0$ Hz, 3H, CH_3), 1.14 (dd, $J = 6.5$, 0.8 Hz, 3H, CH_3), 1.07 (d, $J = 6.2$ Hz, 3H, CH_3), 0.99 (d, $J = 6.2$ Hz, 3H, CH_3). ^{13}C NMR (101 MHz, $CDCl_3$) δ 135.70 (s, 1C, aromatic), 131.78 (s, 2C, aromatic), 128.88 (s, 2C, aromatic), 126.70 (s, 2C, aromatic), 53.34 (s, 1C), 49.58 (s, 1C), 45.27 (s, 1C), 23.23 (s, 1C), 22.88 (s, 1C), 18.01 (s, 1C), 17.30 (s, 1C). EI mass spectrum: *m/z* 223 $[M]^+$ (calculated 223.14 $[M]^+$).

8.8. (R)-2-Phenylthio-N-isopropylpropanamide (8)

To a solution of **7** (786 mg, 6 mmol) in THF (3 mL), diphenyl disulfide (2.62 g, 12 mmol) and tri-*n*-butylphosphine (2.43 g, 12 mmol, 2.95 mL) were added and the reaction mixture was stirred overnight at RT. The solvent was then evaporated. The mixture was then purified by column chromatography using hexane/EtOAc 6/1 as eluent on silica. Rf: 0.31. The evaporation of the solvent gave the pure product as a crystalline solid. Yield: 1.29 g, 97%. ^{1}H NMR (400 MHz, $CDCl_3$) δ 7.32–7.23 (m, 4H, aromatic), 7.22–7.17 (m, 1H, aromatic), 6.36 (s, 1H, NH), 4.03–3.90 (m, 1H, CH), 3.76 (q, $J = 7.3$ Hz, 1H, CH), 1.51 (d, $J = 7.3$ Hz, 3H, CH_3), 1.06 (d, $J = 6.6$ Hz, 3H, CH_3), 0.96 (d, $J = 6.6$ Hz, 3H, CH_3). ^{13}C NMR (101 MHz, $CDCl_3$) δ 170.91 (s, 1C, CO), 134.17 (s, 1C, aromatic), 130.30 (s, 2C, aromatic), 129.24 (s, 2C, aromatic), 127.28 (s, 1C, aromatic), 47.11 (s, 1C, CH), 41.65 (s, 1C, CH), 22.60 (s, 1C, CH_3), 22.49 (s, CH_3), 18.33 (s, CH_3). EI mass spectrum: *m/z* 223 $[M]^+$ (calculated 223.10 $[M]^+$).

8.9. (R)-N-isopropyl-2-(phenylthio)propan-1-amine ((R)-L5)

To a THF solution (11 mL) of compound **8** (620 mg, 2.78 mmol) a THF solution of THF·BH_3 adduct (8.3 mL, 1 M) was added dropwise at 0 °C. (The reaction was performed in an apparatus containing a three necked vessel, a reflux condenser, thermometer and a dropping funnel. The top of the reflux condenser was equipped with a ventilation pipe that was directed into a MeOH bath. Caution! Foaming occurred.) The mixture was then allowed to warm to RT and stirred for 30 min. Then it was refluxed for 5.5 h and cooled to 0 °C. At this temperature 20 mL of MeOH was added and then it was refluxed for an additional 8 h. The solvent was evaporated, 20 mL water was added and the pH of the mixture was adjusted to 2 with dilute HCl solution. It was extracted with 20 mL of ether and the pH of the aqueous phase was adjusted to 12 with Na_2CO_3. It was extracted again with ether (3 × 20 mL), the combined organic phase was dried on $MgSO_4$ and finally the solvent was removed in vacuo. Yield: 469 mg, 81%. ^{1}H NMR (400 MHz, MeOD) δ 7.45–7.39 (m, 2H, aromatic), 7.34–7.22 (m, 3H, aromatic), 3.30 (m, 1H, CH), 2.74 (hept, $J = 6.3$ Hz, 1H, CH), 2.65 (dd, $J = 12.4$, 5.9 Hz, 1H, diast. C*H*H), 2.57 (dd, $J = 12.4$, 7.6 Hz, 1H, diast. CH*H*), 1.27 (d, $J = 6.8$ Hz, 3H, CH_3), 1.03 (d, $J = 6.3$ Hz, 3H, CH_3), 1.01 (d, $J = 6.3$ Hz, 1H, CH_3). ^{13}C NMR (101 MHz, MeOD) δ 134.18 (s, 1C, aromatic), 132.90 (s, 2C, aromatic), 129.05 (s, 2C, aromatic), 127.49 (s, 1C, aromatic), 52.17 (s, 1C), 48.57 (s, 1C), 43.53 (s, 1C), 21.60 (s, 1C), 21.46 (s, 1C), 19.06 (s, 1C). EI mass spectrum: *m/z* 209 $[M]^+$ (calculated 209.12 $[M]^+$).

8.10. (S)-1-(phenylthio)propan-2-amine (9)

Compound **9** was synthesized using the same procedure described for ligand (*S,R*)-**L4**. The crude product was purified by column chromatography by using $CHCl_3$/MeOH 4/1 as eluent on silica. Rf: 0.53. Yield: 42%. ^{1}H NMR (400 MHz, $CDCl_3$) δ 7.40–7.32 (m, 3H, aromatic), 7.29–7.21 (m, 2H, aromatic), 7.19–7.09 (m, 1H, aromatic), 3.18–3.07 (m, 3H, CH and NH_2, overlapped), 3.03 (dd, $J = 13.4$, 5.0 Hz, 1H, diast. C*H*H), 2.87 (ddd, $J = 13.4$, 7.8, 2.2 Hz, 1H, diast. CH*H*), 1.22 (dd, $J = 7.8$, 1.4 Hz, 3H). ^{13}C NMR (101 MHz, $CDCl_3$) δ 135.65 (s, 1C, aromatic), 130.02 (s, 2C, aromatic), 129.14 (s, 2C, aromatic), 126.55 (s, 1C, aromatic), 46.52 (s, 1C, CH), 42.90 (s, 1C, CH_2), 21.90 (s, 1C, CH_3). EI mass spectrum: *m/z* 167 $[M]^+$ (calculated 167.08 $[M]^+$).

8.11. (S)–N-isopropyl-1-(phenylthio)propan-2-amine ((S)-L6)

A mixture of **9** (167 mg, 1 mmol), isopropyl iodide (510 mg, 3 mmol, 299 μL) and K_2CO_3 (76 mg, 0.55 mmol) was stirred for 5 h at 75 °C. The mixture was then purified by column chromathography on silica using $CHCl_3$/MeOH 8/1 as eluent. Rf: 0.45. Yield: 193 mg, 92%.

^{1}H NMR (400 MHz, $CDCl_3$) δ 7.46–7.40 (m, 2H, aromatic), 7.33–7.26 (m, 2H, aromatic), 7.23–7.18 (m, 1H, aromatic), 3.76 (dd, $J = 13.5$, 3.9 Hz, 1H, diast. C*H*H), 3.60–3.47 (m, 1H, CH), 3.44–3.34 (m, 1H, CH), 3.27 (dd, $J = 13.5$, 9.3 Hz, 1H, diast. CH*H*), 1.59 (d, $J = 6.4$ Hz, 3H, CH_3), 1.48 (d, $J = 6.5$ Hz, 3H, CH_3), 1.39 (d, $J = 6.5$ Hz, 3H, CH_3). ^{13}C NMR (101 MHz, $CDCl_3$) δ 133.83 (s, 1C, aromatic), 130.37 (s, 2C, aromatic), 129.49 (s, 2C, aromatic), 127.26 (s, 1C, aromatic), 51.73 (s, 1C), 48.95 (s, 1C), 36.54 (s, 1C), 20.02 (s, 1C), 19.19 (s, 1C), 16.40 (s, 1C). EI mass spectrum: *m/z* 209 $[M]^+$ (calculated 209.12 $[M]^+$).

8.12. N-(2-(phenylthio)ethyl)propan-2-amine (L7)

Compound **L7** was synthesized using the same procedure described for ligand (*S,R*)-**L4** starting from 1-isopropylaminoethanol. Yield: 81%. ^{1}H NMR (400 MHz, MeOD) δ 7.43–7.37 (m, 2H, aromatic), 7.35–7.28 (m, 2H, aromatic), 7.25–7.19 (m, 1H, aromatic), 3.07 (t, $J = 6.9$ Hz, 2H, CH_2), 2.79 (m, 1H, CH), 2.77 (t, $J = 6.8$ Hz, 1H, CH_2), 1.05 (d, $J = 6.3$ Hz, 6H, CH_3). ^{13}C NMR (101 MHz, MeOD) δ 135.41 (s, 1C, aromatic), 129.48 (s, 2C, aromatic), 128.69 (s, 2C), 126.04 (s, 1C, aromatic), 47.90 (s, 1C), 45.22 (s, 1C), 32.64 (s, 1C), 21.10 (s, 2C). EI mass spectrum: *m/z* 195 (calculated 195.11 $[M]^+$).

8.13. (2S,5R)-5-(isopropylamino)hexan-2-ol (10)

A solution of sulfuric acid (20 mL, 20 m/m%) was added to **5** (500 mg, 2.09 mmol) and the mixture was stirred for 8 h at 90 °C. The solution was then allowed to cool to room temperature and its pH was adjusted to 12 by the addition of Na_2CO_3. The aqueous solution was then extracted with ether (3 × 30 mL) and the organic phases were dried with $MgSO_4$. The solvent was evaporated in vacuo to give the title compound as a dense oil. Yield: 142 mg, 43%. ^{1}H NMR (400 MHz, $CDCl_3$) δ 3.78–3.65 (m, 1H, CH), 2.99–2.84 (m, 2H, CH, overlapped), 1.60–1.46 (m, 4H, CH_2, overlapped), 1.14 (d, $J = 6.2$ Hz, 3H, CH_3), 1.08 (d, $J = 6.3$ Hz, 3H, CH_3), 1.07 (d, $J = 6.5$ Hz, 3H, CH_3), 1.06 (d, $J = 6.3$ Hz, 3H, CH_3). ^{13}C NMR (101 MHz, $CDCl_3$) δ 67.06 (s, 1C, CH), 48.97 (s, 1C, CH), 45.51 (s, 1C, CH), 34.67 (s, 1C, CH_2), 33.23 (s, 1C, CH_2), 23.55 (s, 1C, CH_3), 23.12 (s, 1C, CH_3), 22.08 (s, 1C, CH_3), 19.70 (s, 1C, CH_3). EI mass spectrum: *m/z* 159 (calculated 159.16 $[M]^+$).

8.14. (2R,5R)-N-isopropyl-5-(phenylthio)hexan-2-amine ((R,R)-L8)

To a solution of **10** (142 mg, 0.892 mmol) in THF (0.5 mL), diphenyl disulfide (389 mg, 1.78 mmol) and tri-*n*-butylphosphine (360 mg, 1.78 mmol, 438 μL) were added and the reaction mixture was stirred overnight at RT. The solvent was then evaporated, 4 mL of water was added and the pH was adjusted to 2 by using dilute HCl solution. The mixture was extracted with ether (20 mL) and the pH of the aqueous phase was adjusted to 12 with Na_2CO_3. The alkaline solution was then extracted with ether (4 × 20 mL) and the solvent was evaporated in vacuo. To remove the phosphine oxide byproduct the crude mixture was passed through a short pad of

activated Al_2O_3 column by using ether as eluent. The evaporation of the solvent gave the pure product as an oil. Yield: 30 mg, 13%. ^{1}H NMR (400 MHz, MeOD) δ 7.41–7.34 (m, 2H, aromatic), 7.33–7.24 (m, 3H, aromatic), 3.27–3.14 (m, 1H, CH), 3.08–2.95 (m, 1H, CH), 2.88–2.77 (m, 1H, CH), 1.78–1.68 (m, 1H, diast. C*H*H), 1.60–1.51 (m, 1H, CH_2), 1.50–1.41 (m, 1H, diast. CH*H*), 1.26 (d, J = 6.7 Hz, 3H, CH_3), 1.09 (d, J = 6.4 Hz, 3H, CH_3), 1.07 (d, J = 6.3 Hz, 3H, CH_3), 1.04 (d, J = 6.4 Hz, 3H, CH_3). ^{13}C NMR (101 MHz, MeOD) δ 135.56 (s, 1C, aromatic), 132.18 (s, 2C, aromatic), 128.96 (s, 2C, aromatic), 126.96 (s, 1C, aromatic), 50.11 (s, 1C), 45.70 (s, 1C), 43.48 (s, 1C), 32.93 (s, 1C), 32.86 (s, 1C), 21.16 (s, 1C), 20.70 (s, 1C), 20.50 (s, 1C), 18.13 (s, 1C). EI mass spectrum: m/z 251 (calculated 251.17 $[M]^+$).

8.15. [Pd((S,R)-L1)Cl$_2$]

Ligand (*S,R*)-**L1** (50 mg, 0.1752 mmol) dissolved in CH_2Cl_2 (5 mL) was added dropwise to a solution of [Pd(COD)Cl_2] (50 mg, 0.1752 mmol) in CH_2Cl_2. The resulting solution was stirred for 3 h, filtered through a short pad of celite and concentrated to ca. 2 mL. The solution was then treated with ether (5 mL) to precipitate a powder that was filtered and washed with ether (3 × 5 mL) to give 70 mg of complex [Pd((*S,R*)-**L1**)Cl_2]. Yield: 87%. ^{1}H NMR (400 MHz, CD_2Cl_2) δ 8.02–7.92 (m, 2H, aromatic), 7.89–7.79 (m, 2H, aromatic), 7.64–7.58 (m, 2H, aromatic), 7.56–7.43 (m, 4H, aromatic), 3.38 (dqd, J = 8.8, 7.2, 5.0 Hz, 1H, CH), 3.07 (s, 3H, diast. CH_3), 2.92 (s, 3H, diast. CH_3), 2.67 (dqd, J = 38.4, 6.8, 5.3 Hz, 1H, CH), 1.22 (dd, J = 13.2, 7.2 Hz, 3H, CH_3), 1.20 (d, J = 6.7 Hz, 3H, CH_3). ^{13}C NMR (101 MHz, CD_2Cl_2) δ 136.32 (d, J = 11.5 Hz, 2C, aromatic), 132.53 (d, J = 9.1 Hz, 2C, aromatic), 132.44 (d, J = 2.8 Hz, 1C, aromatic), 131.98 (d, J = 3.1 Hz, 1C, aromatic), 129.15 (d, J = 11.1 Hz, 2C, aromatic), 128.53 (d, J = 11.7 Hz, 2C, aromatic), 127.68 (d, J = 56.1 Hz, 1C, aromatic), 125.29 (d, J = 54.2 Hz, 1C, aromatic), 73.72 (d, J = 6.3 Hz, 1C, CH), 52.05 (s, 1C, CH_3), 50.09 (s, 1C, CH_3), 38.87 (d, J = 25.8 Hz, 1C, CH), 13.16 (d, J = 8.3 Hz, 1C, CH_3), 11.27 (d, J = 4.8 Hz, 1C, CH_3). ^{31}P NMR (162 MHz, CD_2Cl_2) δ 50.02 (s). Elemental analysis (%) calcd. for $C_{18}H_{24}Cl_2NPPd$ (462.69): C 46.73, H 5.23, N 3.03; found: C 46.75, H 5.39, N 2.64.

8.16. [Pd((R,R)-L2)Cl$_2$]

Synthesis of complex [Pd((*R,R*)-**L2**)Cl_2] was performed as described for complex [Pd((*S,R*)-**L1**)Cl_2]. Yield: 80%. *Isomer 1:* ^{1}H NMR (400 MHz, CD_2Cl_2) δ 8.19–7.25 (m, 10H, aromatic, overlapped with the corresponding signals of *isomer 2*), 3.60 (m, 1H, CHN)), 3.14 (m, 1H, C*H*(CH_3)$_2$), 2.82 (m, 1H, CHP), 1.61 (d, J = 6.7 Hz, 3H, diast. CH_3(*i*Pr)), 1.43 (d, J = 6.5 Hz, 3H, diast. CH_3(*i*Pr)), 1.32 (d, J = 6.7 Hz, 3H, C*H*$_3$CHN), 0.86 (dd, J = 13.8, 7.0 Hz, 3H, CH_3CHP). ^{13}C NMR (101 MHz, CD_2Cl_2) δ 134.54 (d, J = 11.4 Hz, 2C, aromatic), 132.35 (d, J = 8.7 Hz, 2C, aromatic), 131.68 (d, J = 3.0 Hz, 1C, aromatic), 131.52 (d, J = 2.9 Hz, 1C, aromatic), 128.76 (d, J = 10.8 Hz, 2C, aromatic), 128.11 (d, J = 11.8 Hz, 2C, aromatic), 125.6 (d, J = 53.1 Hz, 1C, aromatic), 125.05 (d, J = 54.0 Hz, 1C, aromatic), 64.84 (d, J = 9.4 Hz, 1C, CHN), 48.44 (s, 1C, C*H*(CH_3)$_2$), 38.27 (d, J = 30.0 Hz, 1C, CHP), 26.91 (d, J = 3.1 Hz, 1C, CH_3(*i*Pr)), 24.18 (s, 1C, CH_3(*i*Pr)), 16.16 (d, J = 19.6 Hz, 1C, *C*H_3CHN), 13.33 (d, J = 6.3 Hz, 1C, *C*H_3CHP). ^{31}P NMR (162 MHz, CD_2Cl_2) δ 52.91 (s). *Isomer 2:* ^{1}H NMR (400 MHz, CD_2Cl_2) δ 8.19–7.25 (m, 10H, aromatic, overlapped with the corresponding signals of *isomer 1*), 3.60 (m, 1H, C*H*(CH_3)$_2$), 3.14 (m, 1H, CHP), 2.59 (m, 1H, CHN), 1.59 (d, J = 6.9 Hz, 3H, diast. CH_3(*i*Pr)), 1.48 (d, J = 6.8 Hz, 3H, diast. CH_3(*i*Pr)), 1.46 (d, J = 6.1 Hz, 3H, C*H*$_3$CHN), 1.10 (dd, J = 13.4, 7.2 Hz, 3H, C*H*$_3$CHP). ^{13}C NMR (101 MHz, CD_2Cl_2) δ 135.66 (d, J = 10.8 Hz, 2C, aromatic), 132.62 (d, J = 9.7 Hz, 2C, aromatic), 131.00 (d, J = 3.4 Hz, 1C, aromatic), 130.94 (d, J = 3.3 Hz, 1C, aromatic), 128.29 (d, J = 11.1 Hz, 2C, aromatic), 128.03 (d, J = 11.9 Hz, 2C, aromatic), 126.69 (d, J = 51.6 Hz, 1C, aromatic), 126.36 (d, J = 53.5 Hz, 1C, aromatic), 59.75 (d, J = 5.3 Hz, 1C, CHN), 55.21 (s, 1C, *C*H(CH_3)$_2$), 46.05 (d, J = 29.0 Hz, 1C, CHP), 23.53 (s, 1C, CH_3(*i*Pr)), 21.42 (s, 1C, CH_3(*i*Pr)), 18.92 (d, J = 18.6 Hz, 1C, *C*H_3CHN), 13.09 (d, J = 7.5 Hz, 1C, *C*H_3CHP). ^{31}P NMR (162 MHz, CD_2Cl_2) δ 61.21 (s). Elemental analysis (%) calcd. for $C_{19}H_{26}Cl_2NPPd$ (476.72): C 47.87, H 5.50, N 2.94; found: C 48.11, H 5.21, N 2.47.

8.17. [Pd((S,R)-L4)Cl$_2$]

Synthesis of complex [Pd((*S,R*)-**L4**)Cl_2] was performed as described for complex [Pd((*S,R*)-**L1**)Cl_2]. Yield: 87%. ^{1}H NMR (400 MHz, CD_2Cl_2) δ 8.08 (d, J = 7.1 Hz, 2H, aromatic), 7.79–7.35 (m, 3H, aromatic), 3.97 (d, J = 5.7 Hz, 1H, NH), 3.64 (m, 1H, CHN), 3.56 (m, 1H, CH(^{i}Pr)), 3.28 (qdd, J = 6.6, 4.4, 0.7 Hz, 1H, CHS), 1.80 (d, J = 6.7 Hz, 3H, diast. CH_3(^{i}Pr)), 1.75 (d, J = 6.7 Hz, 3H, CH_3(S)), 1.53 (d, J = 6.6 Hz, 3H, CH_3(N)), 1.49 (d, J = 6.6 Hz, 1H, diast. CH_3(^{i}Pr)). ^{13}C NMR (101 MHz, CD_2Cl_2) δ 134.08 (s, 2C, aromatic), 132.38 (s, 1C, aromatic), 130.98 (s, 2C, aromatic), 129.60 (s, 1C, aromatic), 62.42 (s, 1C, CH), 60.15 (s, 1C, CH), 55.10 (s, 1C, CH), 25.34 (s, 1C, CH_3), 22.72 (s, 1C, CH_3), 17.14 (s, 1C, CH_3), 15.66 (s, 1C, CH_3).). Elemental analysis (%) calcd. for $C_{13}H_{21}Cl_2NPdS$ (400.70): C 38.97, H 5.28, N 3.50; found: C 38.86, H 5.32, N 3.59.

8.18. [Pd((R)-L5)Cl$_2$]

Synthesis of complex [Pd((*R*)-**L5**)Cl_2] was performed as described for complex [Pd((*S,R*)-**L1**)Cl_2]. Yield: 89%. ^{1}H NMR (400 MHz, CD_2Cl_2) for the major isomer δ 8.31–8.21 (m, 2H, aromatic), 7.66–7.57 (m, 3H, aromatic, overlaps with the aromatic signals of the minor isomer), 6.14 (d, J = 10.5 Hz, 1H, NH), 4.38–4.15 (m, 2H, overlaps with the corresponding signal of the minor isomer, CH), 2.74 (dt, J = 12.5, 3.9 Hz, 1H, diast. C*H*H), 2.62 (q, J = 12.5 Hz, 1H, diast. CH*H*), 1.63 (d, J = 6.7 Hz, 3H, CH_3(*i*Pr)), 1.21 (d, J = 6.9 Hz, 3H, CH_3(*i*Pr)), 1.09 (d, J = 6.8 Hz, 3H, CH_3). ^{1}H NMR (400 MHz, CD_2Cl_2) for the minor isomer δ ^{1}H NMR (400 MHz, CD_2Cl_2) δ 8.17–8.10 (m, 2H, aromatic), 7.56–7.28 (m, 3H, overlaps with the aromatic signals of the major isomer), 6.03 (d, J = 10.5 Hz, 1H, NH), 4.36–4.15 (m, 1H, overlaps with the corresponding signals of the major isomer, CH(*i*Pr)), 4.02 (m, 1H, CH), 2.92 (dt, J = 12.8, 4.7 Hz, 1H, diast. C*H*H), 2.43 (q, 12.8 Hz, 1H, diast. CH*H*), 1.61 (d, J = 6.7 Hz, 3H, CH_3(*i*Pr)), 1.27 (d, J = 6.6 Hz, 3H, CH_3), 1.25 (d, J = 7.0 Hz, 3H, CH_3(*i*Pr)). ^{13}C NMR (101 MHz, CD_2Cl_2) for the major isomer δ 136.31 (s, 2C, aromatic), 132.01 (s, 1C, aromatic), 129.96 (s, 2C, aromatic), 124.68 (s, 1C, aromatic), 52.15 (s, 1C), 51.67 (s, 1C), 48.42 (s, 1C), 20.18 (s, 1C), 20.08 (s, 1C), 13.99 (s, 1C). ^{13}C NMR (101 MHz, CD_2Cl_2) for the minor isomer δ 134.52 (s, 2C, aromatic), 131.68 (s, 1C, aromatic), 130.13 (s, 2C, aromatic), 127.74 (s, 1C, aromatic), 53.49 (s, 1C), 50.28 (s, 1C), 30.07 (s, 1C), 20.33 (s, 1C), 20.18 (s, 1C), 14.88 (s, 1C).). Elemental analysis (%) calcd. for $C_{12}H_{19}Cl_2NPdS$ (386.68): C 37.27, H 4.95, N 3.62; found: C 37.52, H 4.84, N 3.90.

8.19. [Pd((S)-L6)Cl$_2$]

Synthesis of complex [Pd((*S*)-**L6**)Cl_2] was performed as described for complex [Pd((*S,R*)-**L1**)Cl_2]. Yield: 78%. *Isomer 1:* ^{1}H NMR (400 MHz, CD_2Cl_2, 253 K) δ 8.24–7.47 (m, 5H, overlapped with the aromatic signals of the minor isomers), 4.56 (br. s, 1H, NH), 3.52 (dd, J = 13.3, 3.5 Hz, 1H, diast. C*H*H), 3.39–3.27 (m, 2H, CH), 3.03 (dd, J = 13.1, 4.4 Hz, 1H, diast. CH*H*), 1.68 (d, J = 6.6 Hz, 3H, CH_3), 1.65 (d, J = 6.7 Hz, 3H, diast. CH_3), 1.37 (d, J = 6.6 Hz, 3H, diast. CH_3). *Isomer 2:* ^{1}H NMR (400 MHz, CD_2Cl_2, 253 K) δ 8.24–7.47 (m, 5H, overlapped with the aromatic signals of the other isomer), 4.30 (br. s, 1H, NH), 3.55 (m, 1H, diast. C*H*H, partially overlapped with the corresponding signal of the major isomer), 3.48–3.44 (m, 1H, C*H*(CH_3), partially overlapped with the corresponding signal of the

major isomer), 3.43–3.37 (m, 1H, C*H*(CH_3)$_2$, partially overlapped with the corresponding signal of the major isomer), 3.06 (m, 1H, diast. CH*H*, partially overlapped with the corresponding signal of the major isomer), 1.60 (d, J = 6.5 Hz, 6H, CH(CH_3)$_2$), 1.48 (d, J = 6.6 Hz, 3H, CH_3). *Isomer 3*: ^{1}H NMR (400 MHz, CD_2Cl_2, 253 K) δ 8.24–7.47 (m, 5H, overlapped with the aromatic signals of the other isomers), 4.76 (br. m, 1H, NH), 4.14 (m, 1H, C*H*(CH_3)), 3.23 (dd, J = 14.4, 12.8 Hz, 1H, diast. C*H*H), 3.13 (m, 1H, C*H*(CH_3)$_2$), 2.69 (ddd, J = 14.4, 4.1, 1.7 Hz, 1H, diast. CH*H*), 1.93 (d, J = 6.6 Hz, 3H, diast. CH_3), 1.40 (d, J = 6.6 Hz, 3H, diast. CH_3), 1.32 (d, J = 6.7 Hz, 3H, CH_3). ^{13}C NMR (101 MHz, CD_2Cl_2, 293 K) δ 132.75 (br. s, 2C, aromatic), 131.69 (s, 1C, aromatic), 130.93 (br. s, 2C, aromatic), 130.86 (br. s, 1C, aromatic), 58.96 (br. s, 1C), 55.45 (br. s, 1C), 50.18 (br. s, 1C), 24.95 (br. s, 1C), 22.42 (br. s, 1C), 21.26 (br. s, 1C). Elemental analysis (%) calcd. for $C_{12}H_{19}Cl_2NPdS$ (386.68): C 37.27, H 4.95, N 3.62; found: C 37.57, H 4.91, N 3.76.

8.20. [Pd(L7)Cl$_2$]

Synthesis of complex [Pd(**L7**)Cl_2] was performed as described for complex [Pd((*S,R*)-**L1**)Cl_2]. Yield: 95%. ^{1}H NMR (400 MHz, CD_2Cl_2) δ 8.28–8.21 (m, 2H, aromatic), 7.57–7.51 (m, 3H, aromatic), 6.08 (d, J = 10.0 Hz, 1H, NH), 4.24–4.14 (m, 1H, CH(^{i}Pr)), 4.00 (td, J = 13.9, 4.3 Hz, 1H, diast. C*H*H), 2.96 (dtd, J = 12.4, 4.1, 1.4 Hz, 1H, diast. CH*H*), 2.73 (ddd, J = 14.2, 3.5, 1.2 Hz, 1H, diast. C*H*H), 2.62 (ddd, J = 25.1, 12.7, 3.9 Hz, 1H, diast. CH*H*), 1.43 (d, J = 6.7 Hz, 3H, diast. CH_3), 1.19 (d, J = 6.8 Hz, 3H, diast. CH_3). ^{13}C NMR (101 MHz, CD_2Cl_2) δ 132.60 (s, 2C, aromatic), 130.71 (s, 1C, aromatic), 129.98 (s, 2C, aromatic), 129.23 (s, 1C, aromatic), 51.69 (s, 1C), 46.33 (s, 1C), 41.32 (s, 1C), 19.87 (s, 1C), 19.65 (s, 1C). Elemental analysis (%) calcd. for $C_{11}H_{17}Cl_2NPdS\cdot(CH_3)_2CO$ (430.73): C 39.04, H 5.38, N 3.25; found: C 39.22, H 5.23, N 3.64.

References

[1] (a) M.L. Crawley, B.M. Trost (Eds.), Transition Metal Catalysis in the Pharmaceutical Industry, John Wiley & Sons, Inc., New York, NY, 2012;
(b) J. Hagen, Homogeneous catalysis with transition metal catalysts. Industrial Catalysis: A Practical Approach, Wiley-VCH Verlag GmbH & Co. KGaA, 2015.

[2] R.A. Sheldon, I. Arends, U. Hanefeld (Eds.), Green Chemistry and Catalysis, Wiley VCH Verlag GmbH & Co. KGaA, Weinheim, 2007.

[3] J.A. Gillespie, E. Zuidema, P.W.N.M. van Leeuwen, P.C.J. Kamer, Phosphorus ligand effects in homogeneous catalysis and rational catalyst design, in: P.C.J. Kamer, P.W.N.M. van Leeuwen (Eds.), Phosphorus(III) Ligands in Homogeneous Catalysis: Design and Synthesis, John Wiley & Sons, Ltd, Chicester, UK, 2012.

[4] K.C. Harper, E.N. Bess, M.S. Sigman, Nat. Chem. 4 (2012) 366.

[5] S.P. Flanagan, P.J. Guiry, J. Organomet. Chem. 691 (2006) 2125.

[6] (a) G. Farkas, S. Balogh, J. Madarasz, A. Szöllősy, F. Darvas, L. Ürge, M. Gouygou, J. Bakos, Dalton Trans. 41 (2012) 9493;
(b) G. Farkas, Z. Császár, S. Balogh, A. Szöllősy, M. Gouygou, J. Bakos, Catal. Commun. 36 (2013) 94;
(c) C.G. Arena, D. Drommi, F. Faraone, Tetrahedron: Asymmetry 11 (2000) 4753.

[7] (a) K.N. Gavrilov, A.I. Polosukhin, Russ. Chem. Rev. 69 (2000) 661;
(b) V.A. Stepanova, I.P. Smoliakova, Curr. Org. Chem. 16 (2012) 2893;
(c) M.P. Carrol, P.J. Guiry, Chem. Soc. Rev. 43 (2014) 819;
(d) F. Ye, Z.-J. Zheng, L. Li, K.-F. Yang, C.G. Xia, L.W. Xu, Chem. Eur. J. 19 (2013) 15452–15457;
(e) Q.-L. Liu, W. Chen, Q.-Y. Jiang, X.-F. Bai, Z. Li, Z. Xu, L.-W. Xu, ChemCatChem 8 (2016) 1495–1499;
(f) J.-X. Xu, F. Ye, X.-F. Bai, J. Zhang, Z. Xu, Z.-J. Zheng, L.-W. Xu, RSC Adv 6 (2016) 45495–45502.(g) Xu, J.-X.; Ye, F.; Bai, X.-F.; Cui, Y.-M.; Xu, Z.; Zheng, Z.-J.; Xu, L.-W. 2016,6, 70624-70631.

[8] (a) A.M. Masdeu-Bultó, M. Diéguez, E. Martin, M. Gómez, Coord. Chem. Rev. 242 (2003) 159;
(b) H. Pellissier, Tetrahedron 63 (2007) 1297;
(c) M. Mellah, A. Voituriez, E. Schulz, Chem. Rev. 107 (2007) 5133;
(d) H. Pellissier, Chiral Sulfur Ligands: Asymmetric Catalysis, Royal Society of Chemistry, Cambridge, 2009.

[9] (a) J.-B. Xie, J.-H. Xie, X.-Y. Liu, W.-L. Kong, S. Li, Q.-L. Zhou, J. Am. Chem. Soc. 132 (2010) 4538;
(b) S.-F. Zhu, Y.-B. Yu, S. Li, L.-X. Wang, Q.-L. Zhou, Angew. Chem. Int. Ed. 51 (2012) 8872;
(c) J.-B. Xie, J.-H. Xie, X.-Y. Liu, Q.-Q. Zhang, Q.-L. Zhou, Chem. Asian J. 6 (2011) 899;
(d) D.G.I. Petra, P.C.J. Kamer, A.L. Spek, H.E. Schoemaker, P.W.N.M. van Leeuwen, J. Org. Chem. 65 (2000) 3010.

[10] (a) C. Borràs, P. Elías-Rodríguez, A.T. Carmona, I. Robina, O. Pàmies, M. Diéguez, Organometallics 37 (2018) 1682;
(b) M. Magre, M. Biosca, P.-O. Norrby, O. Pàmies, M. Diéguez, ChemCatChem 7 (2015) 4091;
(c) Z. Császár, P. Imre, S. Balogh, A. Bényei, G. Farkas, J. Bakos, Monatsh. Chem. 148 (2017) 2069;
(d) J.-L. Niu, M.-C. Wang, P.-P. Kong, Q.-T. Chen, Y. Zhu, M.-P. Song, Tetrahedron 65 (2009) 8869;
(e) M.M. Major, G. Rövid, S. Balogh, A. Bényei, G. Lendvay, D. Frigyes, J. Bakos, G. Farkas, Appl. Organomet. Chem. 33 (2019) 4726.

[11] (a) M. Wang, L. Liu, Y. Hua, J. Zhang, Y. Shi, D. Wang, Tetrahedron: Asymmetry 16 (2005) 2531;
(b) J.C. Anderson, M. Harding, Chem. Commun. 393 (1998).

[12] (a) Z. Császár, G. Farkas, A. Bényei, G. Lendvay, I. Tóth, J. Bakos, Dalton Trans. 44 (2015) 16352;
(b) G. Farkas, Z. Császár, K. Stágel, E. Nemes, S. Balogh, I. Tóth, A. Bényei, G. Lendvay, J. Bakos, J. Organomet. Chem. 846 (2017) 129.

[13] P.F. Richardson, L.T.J. Nelson, K.B. Sharpless, Tetrahedron Lett. 36 (1995) 9241.

[14] I. Nakagawa, K. Aki, T. Hata, J. Chem. Soc. Perkin Trans. 1 (1983) 1315, 0.

[15] H. Brunner, A. Winter, J. Breu, J. Organomet. Chem. 553 (1998) 285.

[16] (a) A. Albinati, F. Lianza, H. Berger, P.S. Pregosin, H. Rüegger, R.W. Kunz, Inorg. Chem. 32 (1993) 478;
(b) H. Berger, R. Nesper, P. Pregosin, H. Rüegger, M. Wörle, Helv. Chim. Acta 76 (1993) 1520.

[17] R. Romeo, L.M. Scolaro, M.R. Plutino, A. Romeo, F. Nicolo, A. Del Zotto, Eur. J. Inorg. Chem. 629 (2002).

[18] P. Dierkes, P.W.N.M. van Leeuwen, J. Chem. Soc. Dalton Trans. (1999) 1519.

[19] (a) M. Kranenburg, P.C.J. Kamer, P.W.N.M. van Leeuwen, Eur. J. Inorg. Chem. 25 (1998);
(b) R.J. van Haaren, H. Oevering, B.B. Coussens, G.P.F. van Strijdonck, J.N.H. Reek, P.C.J. Kamer, P.W.N.M. van Leeuwen, Eur. J. Inorg. Chem. (1999) 1237.

[20] L. Szi-Ferenc, Z. Császár, G. Lendvay, A. Bényei, S. Balogh, B. Nánási, G. Farkas, J. Bakos, Organometallics 37 (2018) 2203.

[21] G.-Z. Wang, T. Mallat, A. Baiker, Tetrahedron: Asymmetry 8 (1997) 2133.

[22] D. Drew, J.R. Doyle, Inorg. Synth. 13 (1972) 52.